# Evidence for Intermediates during Unfolding and Refolding of a Two-Domain Protein, Phage T4 Lysozyme: Equilibrium and Kinetic Studies†

Michel Desmadril and Jeannine M. Yon*

ABSTRACT: Equilibrium and kinetic studies of the unfolding–refolding of phage T4 lysozyme induced by guanidine hydrochloride are reported. Tryptophan fluorescence and circular dichroism (CD) were used as observables. Several results indicated the existence of intermediates in the unfolded–folded transition, including (1) the noncoincidence of the transition observed by fluorescence and CD, (2) the asymmetry of the transition recorded by CD, and (3) triphasic kinetics, followed by both observables, accounting for the forward and reverse processes. Our data were inconsistent with an independent unfolding or refolding of each domain. They indicated the existence of residual structured regions particularly resistant to denaturant, which involved one or more of the three tryptophans located in the C-terminal domain. Kinetic analysis has made it possible to propose a minimum pathway corresponding to a sequential refolding, with dead-end species arising from an intermediate. We compared our data with the experimental results of Elwell and Schellman [Elwell, M., & Schellman, J. A. (1975) *Biochim. Biophys. Acta 386*, 309–313] and the theoretical analysis of B. Maigret (unpublished results) and proposed that the C-terminal domain refolds first, after which the overall structure can be formed and stabilized.

In many proteins the polypeptide chain, when long enough, folds into several globular units called "domains". The role of domains in the folding process has been particularly emphasized by Wetlaufer (1973, 1982), Yon (1978), Ghélis & Yon (1979, 1982; unpublished results), Janin (1979), Mac Lachlan (1980), and Rossmann & Argos (1980). For several proteins, it has been shown that each domain is able to fold independently. Stable domains have been obtained in the absence of the remainder of the chain for proteins such as elastase (Ghélis et al., 1978; Ghélis, 1980), thioredoxin (Slaby & Holmgren, 1979; Reutiman et al., 1981), serum albumin (Teale & Benjamin, 1976a,b, 1977), and tryptophan synthase (Hogberg-Raibaud & Goldberg, 1977a,b; Zetina & Goldberg, 1980; Milas et al., 1982).

However, in multidomain proteins, even when each is able to fold independently, the presence of the other domains may influence the rate of refolding. In serum albumin (Teale & Benjamin, 1976b, 1977) and in aspartokinase–homoserine dehydrogenase II (Dautry-Varsat & Garel, 1978), it has been shown that isolated domains refold faster than when they are in the entire molecule. By contrast in aspartokinase–homoserine dehydrogenase I (Dautry & Garel, 1981) and in the $\beta$ subunit of *Escherichia coli* tryptophan synthase (Zetina & Goldberg, 1982) the rate constants of the refolding process are not significantly different for the fragments and for the protein. The proportion of intra- and interdomain interactions probably determines the mutual influence of domains for folding and stabilization.

We chose phage T4 lysozyme, a protein devoid of disulfide bridge, to investigate the role of domains in the unfolding and refolding processes. The high-resolution X-ray structure of this protein ($M_r$ 18 300) was achieved by Matthews & Remington (1974) and refined by Remington et al. (1978). It is a two-domain protein: the N-terminal domain (1–71) is from type ($\alpha + \beta$) as defined by Levitt & Chothia (1976), and the C-terminal domain (72–164) is "all-$\alpha$". The two domains are linked by a helical segment, helix 60–79. Although low-angle X-ray scattering data have suggested that phage T4 lysozyme is a "hinge bending enzyme" (Timchenko et al., 1978), it is a rather compact molecule. Attempts to obtain large fragments corresponding to domains have failed (M. Desmadril, M. Tempete-Gaillourdet, O. Amédée-Manesme, G. Crosetti, F. Mennecier, and J. M. Yon, unpublished results). We therefore approached the question through equilibrium studies and kinetic analyses, and our data are reported in the present paper. In certain cases, equilibrium studies of the unfolding–folding transition allow detection of the presence of intermediates. Indeed, a two-state model generally fails (1) when transition curves display more than one plateau or even a shoulder, (2) when transition curves obtained from different observables do not coincide, (3) when $\Delta H$ deduced from a van't Hoff plot is different from $\Delta H$ directly obtained by calorimetric measurements, and (4) when the denaturation or the renaturation process is described by multiphasic kinetics.

Equilibrium studies of guanidine hydrochloride (Gdn·HCl) and temperature-induced denaturation of phage T4 lysozyme and thermosensitive mutants were previously reported by Elwell & Schellman (1975, 1977). They showed that equilibrium transition followed by fluorescence and by circular dichroism was very cooperative and could be interpreted by the two-state approximation. The present study was performed under slightly different conditions: pH 7.4, the optimum for enzymatic activity, was used; this is also the pH value for which the "hinge movement" was suggested by Timchencko et al. (1978). Even at equilibrium, several arguments indicated the occurrence of intermediates, despite the very high cooperativity of the process. Thermodynamic analysis did not indicate that domains unfold and stabilize independently, but residual structures very resistant to denaturation have been observed. Kinetic analyses provided further information on the folding pathway.

Results are discussed in light of data reported by Elwell & Schellman (1975, 1977) and the theoretical approach of B. Maigret (unpublished results).

† From the Laboratoire d'Enzymologie Physico-Chimique et Moléculaire Groupe de Recherche du Centre National de la Recherche Scientifique associé à l'Université de Paris XI, Batiment 430, 91405 Orsay, France. *Received June 3, 1983.* This work has been supported by D.G.R.S.T. (Grant 80.7.0299) in the context of a collaboration between theoreticians (Dr. Maigret and Dr. Premilat) and experimentalists (Dr. Desmadril and Prof. Yon). Dedicated to Professor E. Lederer for his 75th anniversary.

0006-2960/84/0423-0011$01.50/0 

## Materials and Methods

*Enzyme.* Phage T4 lysozyme was prepared from a lysate obtained by infection of 30-L batches of *E. coli* B with phage T4 ac q $e^+$ (wild type); the strain was kindly provided by J. Owen and G. Streisinger (Eugene, OR). The procedure employed was that of Tsugita et al. (1968), slightly modified. For enzyme preparation, rivanol treatment was substituted by RNase plus DNase treatment. Purity of the enzyme was checked by electrophoresis at pH 4.5, under denaturing conditions at pH 8.3, and by chromatography. The extinction coefficient, $\epsilon_{280}$ = 23 900 $M^{-1}$ $cm^{-1}$ (Elwell & Schellman, 1975), was used to evaluate the enzyme concentration.

Enzyme activity was followed by recording the decrease in turbidity of a 0.4 mg/mL suspension of lyophilized *E. coli* in a 50 mM tris(hydroxymethyl)aminomethane (Tris) and 1 mM $MgCl_2$ buffer, pH 7.4, at 23 °C, with either a Cary 14 or a Cary 219 spectrophotometer. An activity unit was defined by a decrease of 0.001 in absorbance per minute at 450 nm from an initial absorbance of 0.6.

*Denaturation–Renaturation.* Denaturation was induced by incubation of T4 lysozyme (final concentration 2 $\mu$M) in various concentrations of Gdn·HCl for 24 h at 23 °C. Renaturation was monitored from T4 lysozyme previously incubated in 6 M Gdn·HCl for 24 h for complete denaturation, then diluted in various mixtures with the final concentration of Gdn·HCl varying from 1.5 to 3 M, and incubated for 24 h according to the temperature (final concentration of protein 2 $\mu$M).

All denaturation and renaturation mixtures in 50 mM Tris-HCl buffer, pH 7.4, contained either 1 mM mercaptoethanol or 100 $\mu$M dithiothreitol (DTT) for circular dichroism measurements. Gdn·HCl concentrations were evaluated from the refractive index by using the tables published by Nozaki (1970).

Before use, all buffer solutions were filtrated on Millipore filters (0.22 $\mu$m), and their intrinsic fluorescence was checked; this was always negligible as was intrinsic ellipticity. Fluorescence was recorded with a Perkin-Elmer P.E. 44 B spectrofluorometer. Circular dichroism was measured with the JOUAN III superdichrograph in Dr. Guschlbauer's laboratory. The temperature was kept constant at ±0.2 °C for all measurements.

*Kinetics of Unfolding and Refolding.* The kinetics of unfolding and refolding were recorded at 23 °C at various final Gdn·HCl concentrations by following either fluorescence intensity at 326 nm (this wavelength corresponded to the maximum difference of the signal between native and denatured protein) or ellipticity at 223 nm, using the same equipment as for equilibrium studies.

For unfolding kinetics, all denaturing solutions were incubated 10 min for temperature equilibration before addition of the enzyme. Denaturing solutions were 50 mM Tris-HCl buffer, pH 7.4, 1 mM $MgCl_2$, 100 $\mu$M DTT, or 1 mM $\beta$-mercaptoethanol with Gdn·HCl final concentration varying from 1.9 to 4 M; zero time corresponded to the addition of the enzyme to the denaturation mixture.

For refolding kinetics, T4 lysozyme was preincubated for 24 h in 6 M Gdn·HCl at 23 °C to complete denaturation. This denatured protein was then diluted in the different regeneration mixtures at zero time. Regeneration mixtures were in 50 mM Tris-HCl buffer, pH 7.4, 1 mM $MgCl_2$, 100 $\mu$M DTT, or 1 mM $\beta$-mercaptoethanol, and the final concentration of Gdn·HCl varied between 1.5 and 2.5 M.

The final concentration of enzyme was 2 $\mu$M for folding as well as for unfolding kinetics, except when the effect of enzyme concentration was checked; in this case, T4 lysozyme concentration varied from 1.1 to 6 $\mu$M. For each experiment, it was verified that final equilibrium was reached by recording the signal after 24 or even 48 h.

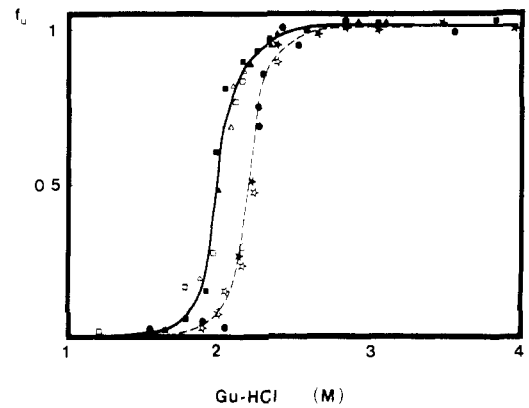


FIGURE 1: Transition curve of T4 lysozyme induced by Gdn·HCl (Gu-HCl) at 23 °C followed by fluorescence emission (---) and variation in circular dichroism at 223 nm (—). Final concentration of protein was 2 $\mu$M in 50 mM Tris-HCl, 1 mM $MgCl_2$, and 1 mM 2-mercaptoethanol (100 $\mu$M DTT for CD measurements) buffer, pH 7.4. Measurements were carried out after a 24-h incubation in different concentrations of Gdn·HCl. (●, ○) Data obtained at equilibrium studied by the shift in maximum fluorescence emission; (■, □) data obtained at equilibrium by using the variation in ellipticity at 223 nm. Also contained in the transition curve are data obtained from kinetic studies, by evaluation of total amplitude when equilibrium is reached. (★, ☆) Results obtained by using variation in fluorescence intensity at 336 nm. (▲, △) Results obtained by using variation in ellipticity at 223 nm. Filled symbols represent unfolding experiments, and open symbols refer to refolding experiments. The fraction of unfolded protein was obtained by using the relation $f_u = (y - y_N)/(y_D - y_N)$ where $y_N$ and $y_D$ are the values of the observable for the native and denatured protein, respectively. The effect of the denaturant on the native and denatured form of T4 lysozyme was considered.

*Analysis of Kinetic Data.* Variations in fluorescence or ellipticity vs. time were analyzed by statistical treatment with a Wang 2200 calculator coupled with a graphic tracer; an iterative multilinear program involving one, two, or three exponential terms was used. Such a treatment allowed the determination of time constants and amplitudes of triphasic kinetics.

*Kinetics Simulation.* Simulation was performed on a Wang 2200 calculator by numerical integration of differential equations derived from kinetic schemes. Since experimentally observed time constants were far apart on the time scale, we used a method described by Kübicek & Visnak (1974), based on an explicit nonlinear algorithm with a program adapted by N. Kellershohn (unpublished data).

## Results

*Reversibility and Cooperativity of the Process.* The denaturation–renaturation transition was studied by fluorescence and circular dichroism (CD). Fluorescence spectra of native and denatured protein at pH 7.4 were similar to those of Elwell & Schellman (1975) at lower pH; the maximum intensity of emission shifted form 326 nm for the native form to 346 nm for the unfolded form, with an increase in fluorescence yield. Figure 1 gives $f_u$ the fraction of unfolded protein, as a function of Gdn·HCl concentration. Identical transition was obtained by following the shift maximum intensity of emission ($\Delta\lambda_{max}$), or variations in fluorescence intensity at 326 nm. For equilibrium studies, we therefore used mainly the shift in $\lambda_{max}$, which gave more accurate measurements. Forward and reverse processes coincided as reported by Elwell and Schellman under slightly different conditions. When the transition was followed

Table I: Cooperativity Index ($n$) and Gdn·HCl Concentration of Half-Transition ($c_m$) for Several Proteins Denatured by Various Procedures

| protein[a] | temp (°C) | pH | denaturant | $c_m$ | coop index $n$ | reference |
|---|---|---|---|---|---|---|
| $T_4L$ | | 5-6 | Gdn·HCl | 2.70 | 16 ± 3 | Elwell & Schellman (1975) |
| $T_4L$ | | 2.5 | temp | | 11 ± 1 | Elwell & Schellman (1975) |
| $T_4L$ | 34.5 | 7.4 | Gdn·HCl | 1.80[b] | 18 ± 3 | |
| $T_4L$ | 28.8 | 7.4 | Gdn·HCl | 2.00[b] | 26 ± 5 | |
| $T_4L$ | 23.0 | 7.4 | Gdn·HCl | 2.25[b] | 23 ± 2 | |
| $T_4L$ | 15.5 | 7.4 | Gdn·HCl | 2.25[b] | 23 ± 2 | |
| HEWL | 30.0 | 5.5 | Gdn·HCl | | 16 | Tanford (1968) |
| lactog | 25.0 | | Gdn·HCl | | 19 | Tanford (1968) |
| lactog | 25.0 | | urea | | 17 | Pace & Tanford (1968) |
| myog | 22.0 | | Gdn·HCl | | 16 | Litman (1966) |
| elastase | 22.0 | 5.4 | Gdn·HCl | 1.60 | 8 ± 1 | Zilber (1979) |
| elastase | 22.0 | 8.0 | Gdn·HCl | 2.60 | 9 ± 1 | Zilber (1979) |
| elastase | 22.0 | 5.4 | urea | 3.80 | 14 ± 1 | Zilber (1979) |
| elastase | 22.0 | 8.0 | urea | 5.90 | 11 ± 1 | Zilber (1979) |

[a] $T_4L$, phage $T_4$ lysozyme; HEWL, hen egg white lysozyme; lactog, lactoglobulin; myog, myoglobin. [b] Fluorescence data.

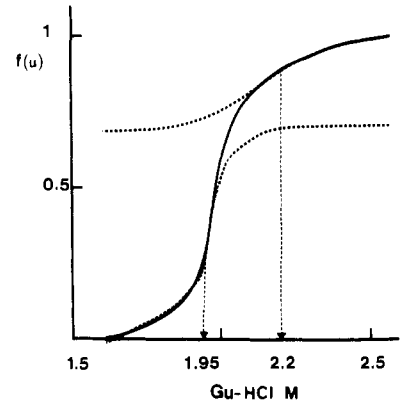


FIGURE 2: Analysis of the CD transition. Transition curve from Figure 1 (—) was broken down into two distinct symmetrical curves. The first one, with a relative amplitude of 70%, had a midpoint of 1.95 M; the second one had a relative amplitude of 30% with a midpoint of 2.2 M.

by circular dichroism at 223 nm, a perfect coincidence in unfolding and refolding processes was also observed. Thus, at pH 7.4 as well at lower pH values, the unfolding–folding transition of T4 lysozyme was reversible when observed by fluorescence and by CD.

Furthermore, the shape of both transitions curves indicated a very high cooperativity in the process. Using a phenomenological treatment proposed by Tanford (1968) and Elwell (1975), we were able to define a cooperativity index $n$, having the same phenomenological meaning as the Hill number:

$$K_{app} = (U)/(N) = f_u/(1 - f_u) = K_0 c^n \qquad (1)$$

with $c$ being the concentration of the denaturant.[1] Table I gives the $n$ of several proteins for transitions induced by temperature and by urea or Gdn·HCl. Compared with other proteins, a very high cooperativity was observed in Gdn·HCl-induced transitions of T4 lysozyme. This cooperativity was higher at pH 7.4 than at lower pH, in agreement with the pH-dependent conformational stability of lysozyme observed by Elwell & Schellman (1975). The high degree of helix content in this protein may have been responsible for the strong cooperativity of the transition.

*Noncoincidence of the Transition Observed by Fluorescence and Circular Dichroism.* Despite the very high cooperativity of the process, transitions observed by fluorescence and by CD

[1] As noted by Tanford, eq 1 should be regarded as an empirical one which is only valid for denaturant concentrations in the transition zone.

Table II: Variations in Ordered Structure Content with Final Concentration of Gdn·HCl

| [Gdn·HCl] (M) | % helix content[a] | % helix remaining folded | % total variation in ellipticity |
|---|---|---|---|
| | 58.0 | 100 | 100 |
| 1.90 | 28.0 | 50 | 80 |
| 2.10 | 12.0 | 21 | 20 |
| 2.15 | 3.8 | 7 | 15 |
| 2.25 | 3.7 | 6 | 10 |
| 2.35 | 0.4 | 1 | 5 |

[a] Helix content was calculated from CD spectra by the procedure of Greenfield & Fasman (1969).

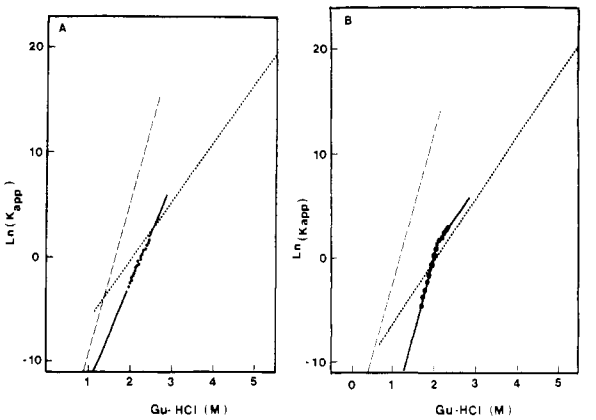


FIGURE 3: Gdn·HCl (Gu-HCl) dependence of $K_{app}$. Data obtained at equilibrium from fluorescence measurements (A) and from CD measurements (B) were compared to the theoretical curve calculated by the procedure of Tanford (---) or by using the values of accessible surface area of each residue (– –) (see text).

at 223 nm did not coincide as shown in Figure 1. The midpoint of the transition curve obtained by fluorescence measurements was 2.20 ± 0.05 M, whereas it was 2.0 ± 0.05 M for the curve obtained by CD measurements.

*Asymmetry of the Transition Followed by CD.* It is noteworthy that the transition observed by CD was asymmetrical. This transition could be resolved in two distinct transition curves (Figure 2). The lower transition curve was strongly cooperative (cooperativity index $n$ = 26) and represented 70% of the total amplitude, with a $c_m$ of 1.9 M. The upper transition, corresponding to 30% of the total amplitude, had a $c_m$ of 2.2 M, approximately identical with the midpoint of the transition curve obtained by fluorescence; it had a lower cooperativity ($n$ = 15). This upper transition corresponded to about 20% of the total helical content of the protein (Table

II). The asymmetry was particularly displayed by the two slopes of the experimental curve in Figure 3B (see below).

These results clearly indicated that the molecule lost part of its ordered structure at a Gdn·HCl concentration lower than that required for changing the tryptophan environment. They therefore revealed the existence of a structured region of the protein more resistant to denaturant than the rest of the molecule. This region contained helical structures and at least one and perhaps more than one of the three tryptophans.

*Dependence of $K_{app}$ upon Denaturant Concentration.* Since T4 lysozyme is a two-domain protein (Remington et al., 1978), we tried to determine whether these intermediates corresponded to independent refolding of each of the two domains, using the same analysis as Rowe & Tanford (1973) for transition of the IgG light chain. First, we calculated the dependency of $K_{app}$ and therefore $\Delta G$, the apparent free energy of unfolding with Gdn·HCl concentration, according to the equation (Schellman, 1978)

$$\frac{\delta \ln K_{app}}{\delta c} = \Delta b_{23}{}^{0} \qquad (2)$$

This experimental value was compared with the predicted value obtained from the free energy of transfer of the amino acids in a given denaturant (Tanford, 1970; Pace, 1975):

$$\delta\Delta G = \sum_{i}^{n} n_i \Delta\alpha_i \Delta g_{itr} \qquad (3)$$

with $\delta\Delta G$ being the variation of free energy due to variations in interactions with the solvent, $n_i$, the number of residues from type $i$, $\Delta g_{itr}$, their corresponding contribution to the free energy of transfer, and $\Delta\alpha_i$, a factor taking into account the difference in accessibility of these groups in the native and unfolded forms.

For a two-domain protein, when each domain represented about half of the whole protein, the experimental value of $\Delta b_{23}{}^{0}$ was half of the calculated one (Rowe & Tanford, 1973; Tanford, 1970).

We attempted the same approach for phage T4 lysozyme. Two different sets of values were used for the evaluation of $\Delta b_{23}{}^{0}$: on the one hand, an average value of $\Delta\alpha$ equal to 0.325, as given by Tanford (1970), and, on the other, $\Delta\alpha$ calculated for each residue from the variation in accessible surface area in native and denatured protein with values given by J. Janin (personal communication) and by Chothia (1976). Results are indicated in Figure 3. The experimental slopes were larger than those calculated according to Tanford. This was surprising, but the empirical parameters proposed by Tanford (1968) were approximate values; $\Delta\alpha_i$ values were averaged and did not take into account the particular structure of individual proteins or the different degrees of exposure of each amino acid in the native structure. For phage T4 lysozyme, the high content in $\alpha$ helix (60% of the molecule) and consequently the large number of peptide bonds included in the ordered structures may have caused the theoretical values to be underestimated by using Tanford's value of $\Delta\alpha$.

A direct calculation of the variation in accessibility of each residue based on X-ray data was more accurate than the preceding estimation. In this case, the experimental slope was smaller than that obtained from the difference in accessible surface area calculated for each residue. The difference observed between experimental and expected slope indicated the existence of intermediates, but since the experimental slope was not equal to half of the theoretical one, even when calculated on the basis of the real structure of T4 lysozyme, we could not conclude that there was an independent refolding–unfolding of each domain. From circular dichroism measurements, two different values of $\Delta b_{23}{}^{0}$ were obtained, reflecting the asymmetry observed in the transition curve; thus, the variation in $K_{app}$ with the denaturant concentration could not be easily analyzed.

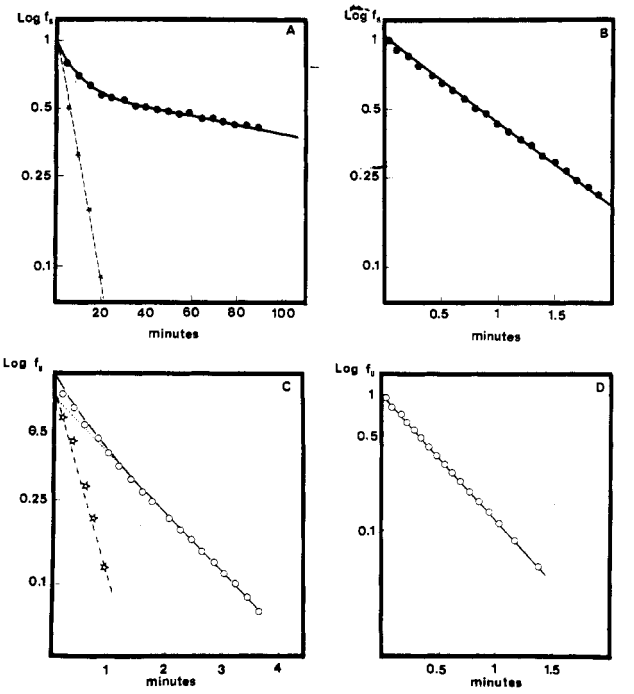


FIGURE 4: Kinetics of the forward and reverse transition of T4 lysozyme induced by Gdn·HCl followed by fluorescence intensity. Experimental conditions were the same as in Figure 1. For refolding kinetics, T4 lysozyme was previously incubated for 24 h in 6 M Gdn·HCl before dilution in regeneration mixture. Semilog plots of denaturation kinetics in 2.2 (A) and 1.8 M (B) final concentration of Gdn·HCl. Semilog plot of renaturation kinetics in 2.18 (C) and 2 M (D) Gdn·HCl final concentration.

*Kinetics Followed by Variation in Fluorescence Intensity at 326 nm.* The unfolding process could be described up to a first approximation by biphasic kinetics in a large range of Gdn·HCl concentrations; a slow phase followed a rapid phase, with the time constant of the slower phase being at least 2 orders of magnitude smaller depending upon the Gdn·HCl final concentration. For high values of Gdn·HCl concentration, i.e., above the transition zone, essentially monophasic kinetics were observed. This indicates that other phases had low amplitudes under these conditions, taking into acount the total amplitude observed at equilibrium.

Similarly the kinetics of refolding could be analyzed as the sum of two exponential terms, one with a time constant comparable to that of the rapid phase of the unfolding process and the other with a larger time constant. When Gdn·HCl concentrations were below the transition zone, only one phase was observed. These results are summarized in Figure 4 and Table III.

In the transition region, the refolding process was much faster than the unfolding process so that in some experiments it was not possible to measure the fastest phase: it had a very small amplitude and a time constant too large to be observed under our experimental conditions (mixing requires about 10 s). It was verified that this rapid phase was not an artifact, corresponding, for example, to the fact that the mixture was not yet homogeneous at the early time of recording. Indeed, when T4 lysozyme, previously unfolded in 6 M Gdn·HCl, was added to a 4 M Gdn·HCl solution (which is also a concentration at which lysozyme was totally unfolded), no variation in the signal was detected. Moreover, the sum of the different

Table III: Macroscopic Constants and Associated Relative Amplitudes of Denaturation–Renaturation Kinetics Monitored by Fluorescence at 23 °C[a]

| final concn of Gdn·HCl (M) | kinetics | $\lambda_1$ ($min^{-1}$) | $\lambda_2$ ($min^{-2}$) | $A_1$ | $A_2$ |
|---|---|---|---|---|---|
| 1.9 | U → N | 4.60 | | 1.00 | |
| 2.0 | U → N | 2.20 | | 1.00 | |
| 2.1 | U → N | 4.30 | 1.20 | 0.33 | 0.64 |
| 2.2 | U → N | 1.30 | 0.55 | 0.38 | 0.62 |
| 2.2 | N → U | 0.25 | $5.5 \times 10^{-3}$ | 0.11 | 0.89 |
| 2.3 | U → N | 0.30 | | 1.00 | |
| 2.3 | N → U | 0.50 | $7.0 \times 10^{-3}$ | 0.17 | 0.83 |
| 2.4 | U → N | 0.22 | | 1.00 | |
| 2.4 | N → U | 0.17 | $1.5 \times 10^{-2}$ | 0.24 | 0.76 |
| 2.6 | N → U | 0.12 | $5.0 \times 10^{-3}$ | 0.40 | 0.60 |
| 2.7 | N → U | 0.16 | $1.0 \times 10^{-2}$ | 0.73 | 0.27 |
| 2.8 | N → U | 0.22 | | 1.00 | |
| 3.0 | N → U | 0.50 | | 1.00 | |
| 3.5 | N → U | 0.90 | $2.0 \times 10^{-2}$ | 0.95 | 0.95 |
| 3.9 | N → U | 3.00 | | 1.00 | |

[a] Signal was analyzed with the equation $(f_{(t)} - f_\infty)/(f_0 - f_\infty) = A_1 e^{-\lambda_1 t} + A_2 e^{-\lambda_2 t}$.

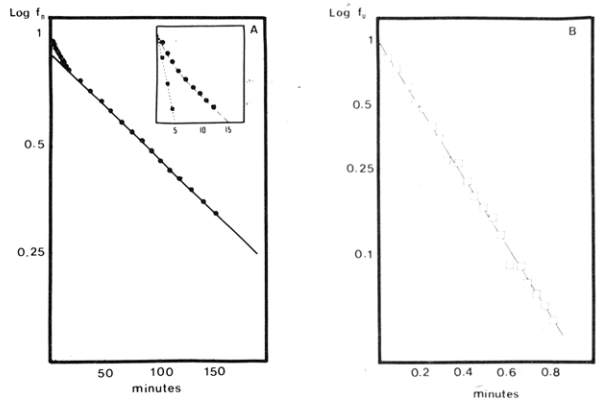


FIGURE 5: Kinetics of Gdn·HCl-induced transition observed by variation in ellipticity at 223 nm. Experimental conditions were identical with those of Figure 4 except that 100 $\mu$M DTT was added instead of 1 mM 2-mercaptoethanol. (A) Semilog plot of unfolding kinetics in 2.34 M Gdn·HCl final concentration. (Insert) Residual plot after subtraction of exponential term corresponding to the slow phase. (B) Semilog plot of refolding kinetics in 2.2 M Gdn·HCl final concentration.

phases corresponded to the amplitude obtained from the equilibrium experiments.

*Kinetics Followed by Variation in Ellipticity at 223 nm.* At 23 °C the kinetics of unfolding could be described by three exponential terms (Figure 5A). The slow phase was similar to the slow phase detected by fluorescence; it had comparable time constants and relative amplitudes (Table IV). This slow phase therefore corresponded to the unfolding of the part of the chain which contained ordered structures and at least one of the three chromophoric groups. Two rapid phases were observed, with the apparent rate constant of the fastest phase corresponding to that of the very rapid refolding phase observed by fluorescence.

In refolding experiments, all kinetics could be analyzed with a single exponential term (Figure 5B).

*Analysis of the Kinetic Phases. (A) Analysis of the Slow Phase Observed for the Unfolding Process.* Unfolding is a slow process and can described by two exponential terms with the second phase being very slow. The slow phase has been observed by fluorescence as well as by CD measurements. It has been reported by Nall et al. (1978) that a slow reaction due to aggregation might occur for Gdn·HCl concentrations in the transition zone. For T4 lysozyme, several points argued against the possibility of aggregation being responsible for the slower phase: (1) Kinetics performed at various protein concentrations (from 1.9 to 6 $\mu$M) indicated that the rate was not dependent on protein concentration. (2) The sum of the amplitudes of the different phases was equal to the amplitude observed at equilibrium for both unfolding and refolding processes. (3) The time constant of the slow phase did not depend upon initial conditions; the same results were obtained whether unfolding was performed with a totally native or partially unfolded protein (obtained by incubation in 1, 1.5, or 2 M Gdn·HCl). (4) During the unfolding process, we always observed a decrease in fluorescence intensity. Furthermore, we detected that light scattering was perfectly negligible. (5) All experiments were performed under reducing conditions to avoid intermolecular disulfide bridge formation (1 mM $\beta$-mercaptoethanol or 100 $\mu$M DTT). (6) Artifacts due to photolysis or adsorption on quartz were not responsible for the slow phase. Both kinds of artifacts could be dismissed by the same experiments. Several kinetics were performed in solutions kept in plastic tubes, aliquots were taken at various times, and fluorescence was measured. Kinetics obtained in this way were superimposable on those which had been directly recorded. (7) For the refolding process, 100% of the initial activity was recovered, whatever the initial conditions. (8) The amplitude of the slow phase was Gdn·HCl concentration dependent (see Table IV). However, the physical meaning of slow phase having a time constant greater than that observed for most small proteins is difficult to ascertain.

*(B) Analysis of the Fastest Phase of Denaturation.* Several arguments indicated that the fastest phase was not an artifact due to the time required for making mixtures homogeneous: (1) this phase was not observed for renaturation, (2) it was Gdn·HCl dependent, and (3) the sum of the amplitudes of each phase was equal to the total amplitude variations observed under equilibrium conditions for the same Gdn·HCl final conditions.

Table IV: Macroscopic Constants and Associated Relative Amplitudes of Unfolding–Refolding Kinetics[a]

| final concn of Gdn·HCl (M) | kinetics | $\lambda_1$ ($min^{-1}$) | $\lambda_2$ ($min^{-1}$) | $\lambda_3$ ($min^{-1}$) | $A_1$ | $A_2$ | $A_3$ |
|---|---|---|---|---|---|---|---|
| 1.90 | U → N | 1.07 | | | 1 | | |
| 2.00 | N → U | 0.03 | | $2 \times 10^{-3}$ | 0.07 | | 0.93 |
| 2.10 | U → N | 0.40 | | | 1 | | |
| 2.15 | U → N | 0.36 | | | 1 | | |
| 2.20 | U → N | 0.28 | | | 1 | | |
| 2.25 | N → U | 3.00 | 0.15 | $5 \times 10^{-3}$ | 0.01 | 0.12 | 0.87 |
| 2.34 | N → U | 1.20 | 0.05 | $6 \times 10^{-3}$ | 0.02 | 0.08 | 0.90 |
| 2.40 | N → U | | 0.42 | 0.024 | | 0.35 | 0.65 |
| 2.70 | N → U | 0.12 | | | 1 | | |
| 3.00 | N → U | 0.30 | | | 1 | | |

[a] Signal was CD, and experimental data were analyzed with the equation $(E_{(t)} - E_\infty)/(E_0 - E_\infty) = A_1 e^{-\lambda_1 t} + A_2 e^{-\lambda_2 t} + A_3 e^{-\lambda_3 t}$.

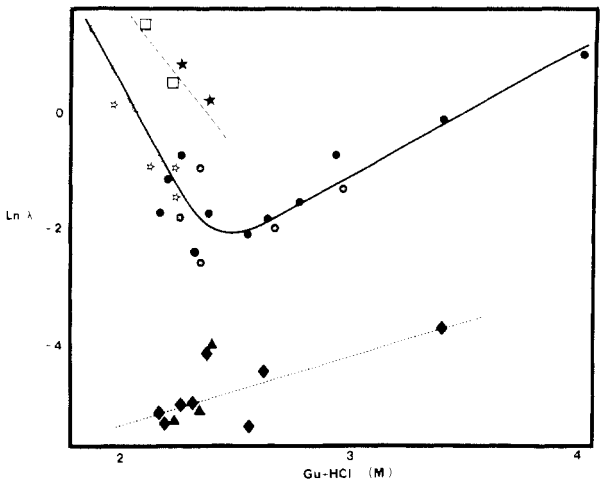


FIGURE 6: Variations in macroscopic rate constants obtained by variation in fluorescence and CD with Gdn·HCl concentration: slow phase of denaturation observed by variation in fluorescence intensity (♦) and variation in ellipticity at 223 nm (▲); fast phase of denaturation observed by variation in fluorescence intensity (●) and variation in ellipticity at 223 nm (open star in filled circle); very fast phase of denaturation observed by ellipticity at 223 nm (★); renaturation phase observed by fluorescence intensity (○) and CD at 223 nm (☆); very fast phase observed by fluorescence intensity (□).

(*C*) *Analysis of the Slow Phase of Renaturation.* To check for aggregation, we measured the ellipticity at the end of each experiment when the signal had reached its equilibrium value, and 6 h later. Variations observed after this time were less than 5% of the total amplitude, excluding a possible artifact due to aggregation.

*Analysis of Kinetic Data.* Since the λ values must be identical for the forward and reverse processes, kinetics of T4 lysozyme unfolding–refolding could be reasonably described by the sum of three exponential terms:

$$f = P_1 e^{-\lambda_1 t} + P_2 e^{-\lambda_2 t} + P_3 e^{-\lambda_3 t}$$

with $f$ being the fraction of unfolded or refolded protein, $\lambda_i$, the macroscopic rate constants, and $P_i$, the amplitudes of the exponential phase $i$. These amplitudes were different for the folding and the unfolding processes.

The variations in the time constants with Gdn·HCl concentration are illustrated in Figure 6, and variations in relative amplitudes with Gdn·HCl concentration are shown in Figure 7 for both fluorescence and CD signals.

Taking into account the values of the rate constants and amplitudes, we tried to determine the best scheme for the unfolding–refolding pathway. We examined different schemes and used the diagnostic rules proposed by Ikai & Tanford (1973) and by Hagerman (1977). Since these rules were not completely unambiguous, we also compared simulated curves derived from different schemes to the experimental kinetics.

Various models were analyzed. The first involved an independent refolding of the domains. Since T4 lysozyme was a two-domain protein, we first checked the possibility of independent refolding of each of the domains (model I). The following scheme, which involved four species, was proposed by Rowe & Tanford (1973) for the independent refolding of domains in the immunoglobulin G light chain:

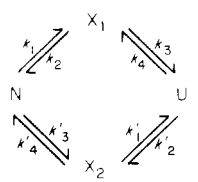


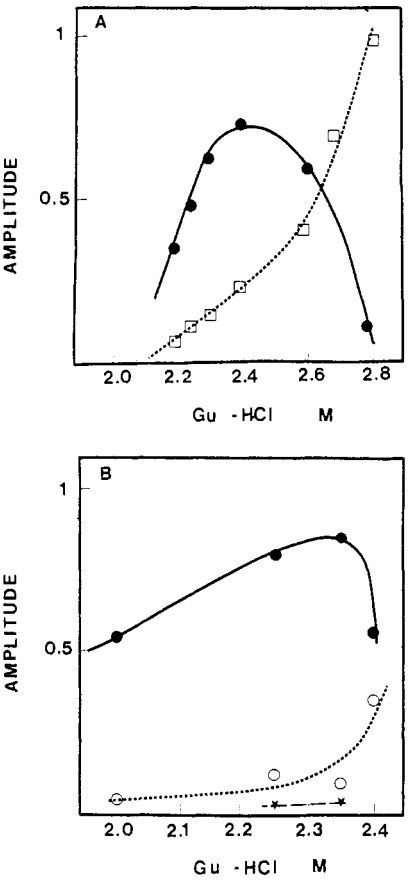


FIGURE 7: Variations in corresponding amplitudes with Gdn·HCl concentrations. (A) Fluorescence measurements: (□) slow phase and (●) fast phase. (B) Ellipticity measurements: (●) slow phase, (○) fast phase, and (★) very fast phase.

In this scheme, $X_1$ represents species in which the first domain, but not the second, is folded; conversely, $X_2$ refers to species in which the second domain is folded, but not the first. When domains fold independently, all $k'_i$ are equal to $k_i$. Such a scheme may be described by two exponential terms with the macroscopic rate constants:

$$\lambda_1 = k_1 + k_2$$

$$\lambda_2 = k_3 + k_4$$

In such a case, each domain is associated with a fraction $\alpha_1$ and $1 - \alpha_1$ of the observable. It can be shown (Ikai & Tanford, 1973) that this model requires the amplitudes associated with each phase to be constant below and above the transition zone. Figure 7 indicates that the ratio of the two amplitudes varies with Gdn·HCl concentration. Therefore, this mechanism does not apply to unfolding–refolding of the T4 lysozyme, as also shown from equilibrium data. A more complex mechanism must be proposed.

We therefore tested the same scheme, but with a dependent refolding of the domains: if $k'_i \neq k_i$ (model II) and if we assumed that $X_1$ and $X_2$ do not accumulate sufficiently to affect the kinetics in the transition zone. Indeed, for Gdn·HCl-induced transition of hen egg white lysozyme, Tanford et al. (1973) found biphasic kinetics at very low and at very high concentrations of Gdn·HCl and monophasic kinetics in the transition zone. The same data, however, were reevaluated, and another interpretation was proposed involving the occurrence of two species under initial conditions (Hagerman, 1977). For T4 lysozyme we have observed a completely different behavior, i.e., multiphasic kinetics only in the transition zone; therefore, model II could not account for our data.

We examined several models involving four species and a side reaction. These models took into account triphasic kinetics exhibiting different amplitudes for reverse and forward reactions:

model III

$$X_2 \underset{k_6}{\overset{k_5}{\rightleftharpoons}} N \underset{k_2}{\overset{k_1}{\rightleftharpoons}} X_1 \underset{k_4}{\overset{k_3}{\rightleftharpoons}} U$$

model IV

$$N \underset{k_2}{\overset{k_1}{\rightleftharpoons}} X_1 \underset{k_4}{\overset{k_3}{\rightleftharpoons}} U \underset{k_6}{\overset{k_5}{\rightleftharpoons}} X_2$$

model V

$$N \underset{k_2}{\overset{k_1}{\rightleftharpoons}} X_1 \underset{k_4}{\overset{k_3}{\rightleftharpoons}} U$$
$$k_6 \uparrow\downarrow k_5$$
$$X_2$$

The validity of these three different schemes was checked by simulating kinetics and by optimizing time constants and the fraction of the signal corresponding to intermediates. The sum of molar fraction of all species is given by

$$f_U + f_{X_1} + f_{X_2} + f_N = 1$$

The observed signal, $y$, is the sum of the contributions of each species multiplied by a coefficient characteristic of the properties of these species (molar ellipticity of fluorescence):

$$y = r_U(U) + r_{X_1}(X_1) + r_{X_2}(X_2) + r_N(N)$$

Various simulations were performed for the three models by varying intrinsic rate constants and $r$ values by using the procedure of Kübicek and Visnak. For model III, it was not possible to find values that fit the experimental data. Model IV, involving dead-end species in equilibrium with the denatured forms (two denatured forms, as shown for ribonuclease; Garel & Baldwin, 1973), were examined. Simulations generated behavior similar to the experimental one for denaturation, but not for the renaturation process. The slow phase experimentally observed for denaturation but not for renaturation appeared in simulation for both reactions. No set of parameters led to simulated kinetics identical with the experimental ones. The best fit with experimental data was obtained by simulation of model V using values of 0.4 and 0.6 for $r_{X_1}$ and $r_{X_2}$, respectively. Such a model accounted for triphasic kinetics in the denaturation process and biphasic kinetics in the refolding process, as experimentally observed.

*Accuracy of Model V.* To check the relevance of model V, we performed two kinds of experiments and compared the results with data obtained by simulation of the same experiments according to model V. In the first set of experiments, the kinetics of refolding were followed during a double jump of Gdn·HCl concentration. In the second set of experiments, unfolding was obtained beginning with different Gdn·HCl concentrations in the transition zone.

*(A) Kinetics of Refolding with a Double Jump in the Gdn·HCl Concentration.* At time zero, T4 lysozyme (at a final concentration of 2 μM) was added to a 2.5 M Gdn·HCl solution, which induced complete unfolding of the molecule under these conditions. Kinetics of unfolding were slow enough to be studied. At a given time, aliquots were withdrawn and placed into a regeneration mixture containing 1.5 M Gdn·HCl final concentration. The kinetics of refolding were followed by using the variation in fluorescence intensity at 336 nm. All kinetics were analyzed by a single exponential term and exhibited identical λ values (Table V). This experiment was reproduced by simulation of model V. Starting at different points of the denaturation curve, the kinetics of refolding were simulated; Figure 8 illustrates the results. Rate constants thus obtained are also indicated in Table V. As in the experiments, the rate constants resulting from simulations did not depend upon the starting points. A satisfactory agreement was obtained between the experimental values and those obtained from simulation.

Table V: Macroscopic Constants of Experimental and Simulated Kinetics for Double-Jump Gdn·HCl Experiments[a]

| denaturation time | $\lambda_1$ ($min^{-1}$), experimental | $\lambda$ ($min^{-1}$), simulated |
|---|---|---|
| 5 | 0.34 | 0.46 |
| 10 | 0.40 | 0.43 |
| 20 | 0.36 | 0.41 |
| 30 | 0.40 | |
| 45 | | 0.40 |
| 60 | 0.46 | |
| 70 | | 0.39 |
| 120 | 0.45 | 0.38 |

[a] Calculations were performed with movel V by using the following microscopic constants: $k_1 = 0.5\ min^{-1}$; $k_2 = 7 \times 10^{-3}\ min^{-1}$; $k_3 = 0.6\ min^{-1}$; $k_4 = 5 \times 10^{-3}\ min^{-1}$; $k_5 = 3 \times 10^{-3}\ min^{-1}$; $k_6 = 0.45\ min^{-1}$.

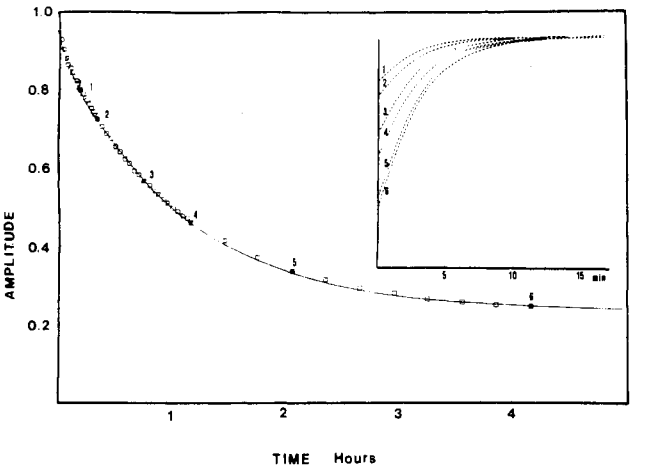


FIGURE 8: Simulation of kinetics of refolding according to model V. The main curve simulated typical kinetics of denaturation with the following constant values: $k_1 = 0.7\ min^{-1}$, $k_2 = 0.2\ min^{-1}$, $k_3 = 2 \times 10^{-3}\ min^{-1}$, $k_4 = 3 \times 10^{-2}\ min^{-1}$, $k_5 = 1 \times 10^{-3}\ min^{-1}$, and $k_6 = 5 \times 10^{-3}\ min^{-1}$. Insert shows stimulated kinetics of refolding from the different points indicated in the denaturation curve.

*(B) Kinetics of Unfolding Starting from Different Initial Conditions of Gdn·HCl Concentration along the Transition Zone.* In this set of experiments, we first incubated T4 lysozyme in different Gdn·HCl concentrations in the transition zone; we then followed the kinetics of unfolding in 3 M Gdn·HCl by fluorescence intensity at 336 nm. The final concentration of protein was 2 μM. These same experiments were simulated, and the λ values obtained from experimental and simulated kinetics are quoted in Table VI. As with previous results, there was good agreement.

## Discussion

On the basis of equilibrium data, and despite the particularly high cooperativity of the process, probably due to the helix content of the protein, evidence was obtained for the occurrence of intermediates in the transition of T4 lysozyme induced by Gdn·HCl at pH 7.4 (1) A noncoincidence of transition curves obtained from two different observables was observed including variations in fluorescence $\lambda_{max}$ and a variation in ellipticity at 223 nm. (2) The transition followed by CD at

Table VI: Macroscopic Constants of Experimental and Simulated Kinetics for Renaturation under Various Initial Conditions[a]

| N/U apparent initial ratio | λ ($min^{-1}$), experimental | λ ($min^{-1}$), simulated |
|---|---|---|
| 0.010 | 0.47 | |
| 0.026 | 0.47 | |
| 0.149 | 0.51 | |
| 0.252 | | 0.50 |
| 0.351 | | 0.52 |
| 0.493 | 0.52 | |
| 0.771 | | 0.51 |
| 1.184 | | 0.51 |
| 2.45 | 0.49 | 0.46 |

[a] Calculations were performed with model V by using the following microscopic constants: $k_1 = 7 \times 10^{-3}$ $min^{-1}$; $k_2 = 1$ $min^{-1}$; $k_3 = 5 \times 10^{-3}$ $min^{-1}$; $k_4 = 0.5$ $min^{-1}$; $k_5 = 2 \times 10^{-2}$ $min^{-1}$; $k_6 = 5 \times 10^{-3}$ $min^{-1}$.

223 nm was asymmetric and able to be decomposed in two separate transitions. (3) Although this argument was more indirect, thermodynamic behavior (as for example, variations in ln $K_{app}$ vs. Gdn·HCl concentration) was incompatible with a two-state process, and these data were corroborated by kinetic studies. (4) Under various conditions of denaturant concentrations the unfolding–refolding of of T4 lysozyme was a complex process which could be described by three exponential terms, for both the forward and reverse reactions. Thus, at least four species were involved in the process.

The quantity of the intermediates at equilibrium seemed strongly pH dependent since, at lower pH (even pH 5 or 6), Elwell & Schellman (1975, 1977) were able to interpret their results according to a two-state approximation. These intermediates, negligible at lower pH, became significantly populated when the pH reached its maximum value for the activity of the enzyme and then became detectable even from equilibrium studies.

Although no direct information is available, the nature of the intermediates can be discussed from data presented in this paper. A comparison of transition curves obtained by fluorescence and CD measurements clearly indicates that part of the molecule, that which contains the tryptophans, i.e., the region located in the C-terminal domain, unfolds at higher concentrations of denaturant than the rest of the molecule. This structured region contains 20% of the entire helix content of T4 lysozyme. These results can be compared with those obtained by Elwell & Schellman (1977) on mutant enzymes. The single change of Trp-138 → Tyr-138 has a considerable effect on the stability of the enzyme, leading a change in $\Delta H$ representing 20% of the entire $\Delta H$ of molecule unfolding. Furthermore, in the three-dimensional structure of T4 lysozyme, only Trp-138 is totally buried in the native protein, with the other two Trp only partially buried (Figure 9). This information suggests that Trp-138 is part of a nucleation center of the protein. Through evaluation of the surface area buried on contact between residues, B. Maigret (unpublished results) has recently shown that Trp-138 strongly interacts with Met-102 and Met-106, which are part of helix 95–106. This nucleation center is probably formed upon hydrophobic interactions of Trp-138 with Met-102; indeed, hydrophobicity was proposed as the driving force for nucleation (Matheson & Scheraga, 1978) as previously suggested by Kauzmann (1959). Furthermore, Trp-138 is included in a short helical segment (Arg-137–Asn-140), with Arg-137 interacting with the Glu-22 of β-segment 18–34 from the N-terminal domain. Through the same procedure, B. Maigret has also shown that

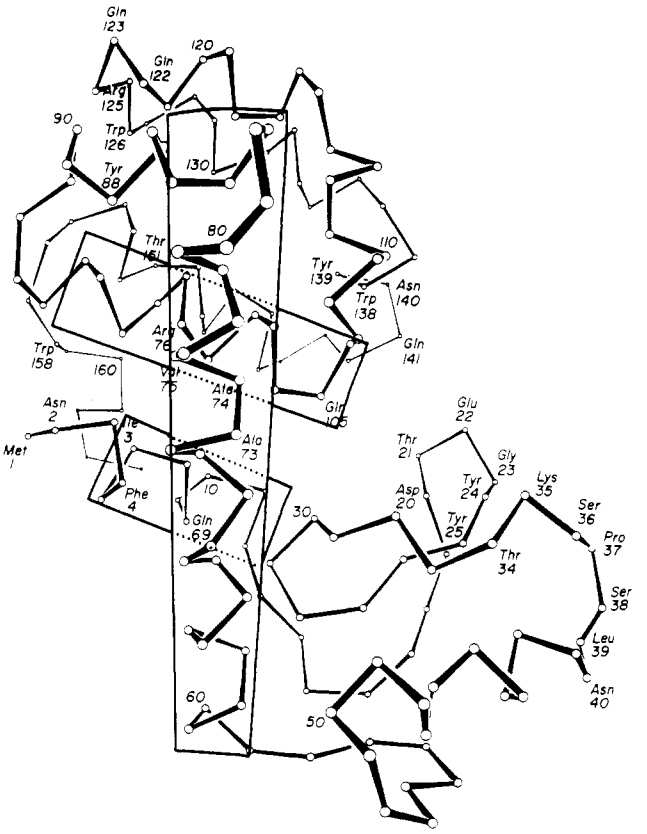


FIGURE 9: Three-dimensional ribbon structure of T4 lysozyme reproduced from B. Matthews (with courtesy of the author). The three interaction helices are indicated.

the stability of the overall structure is ensured by the interaction of three helical segments, helix 3–11, helix 60–79, and helix 95–106. Kinetic studies suggest model V as a plausible one for describing the folding pathway of T4 lysozyme. It probably represents a minimum pathway; other, more unstable species may occur during the refolding of the protein but are undetectable under our conditions. We tested only a few models and do not claim that model V is the only one which may account for the results. Further data are necessary to improve a model, and although it may be phenomenologically valid, the nature of intermediates $X_1$ and $X_2$ can only be hypothesized. The occurrence of two unfolded forms as with ribonuclease (Garel & Baldwin, 1973) is incompatible with our data. $X_1$ represents a partially folded species in which at least one of the three tryptophans is buried; $X_2$ represents a dead-end species and can be assumed to be partially folded.

The fact that $\lambda_2$ has a minimum value located between the midpoint and the end of the transition may result from the formation of dead-end species $X_2$. It may represent a kinetic "through" comparable to the "through" observed under equlibrium conditions for β-galactosidase (Goldberg, 1972), for tryptophanase (London et al., 1974), and for tryptophan synthase (Zetina & Goldberg, 1980) and for elastase (C. Ghélis and E. Zilber, unpublished results). In T4 lysozyme, such a "through" is not observed under equilibrium conditions (M. Desmadril et al., unpublished results); transformation of $X_2$ into $X_1$ is fast enough, and there is no further irreversible or slowly reversible transformation of $X_2$ into other species. It is only observed by kinetic studies. Another explanation for the occurrence of such a minimum in the macroscopic rate constant was proposed by Hagerman & Baldwin (1976) for thermal denaturation–renaturation; the authors emphasized similarities with the behavior of the α-helix formation and proposed that the existence of a minimum is an indication of

nucleation-dependent reactions.

Neither kinetic data nor equilibrium studies are consistent with the independent folding of each domain but rather suggest a sequential renaturation. It is plausible that the region around this Trp-138 folds in earlier steps of T4 lysozyme folding. A partially refolded intermediate is then formed, containing structured segment (137–140); perhaps at this stage, parts of the segment around either Trp-126 or Trp-158, or both, regain their structure, since fluorescence changes are correlated only with the last 40% ellipticity change. It is reasonable to propose that the C-terminal domain refolds prior to the N-terminal one, with an intermediate species being this C-terminal domain, partially or totally refolded. In this protein, the two domains depend strongly on their mutual interactions for stability. Further data are needed to understand how T4 lysozyme reaches its active conformation. Computation studies are now under way in Maigret's laboratory to propose a plausible pathway of unfolding based on structural data.

Acknowledgments

We are indebted to Dr. J. Schellman, Dr. C. Ghélis, and Dr. J. Janin for helpful discussions and Dr. M. Goldberg and R. L. Baldwin for carefully reading the manuscript. We want to thank Dr. Streisinger and Dr. J. Owen for providing the strain of phage T4 and Dr. J. Legault-Demare for his kind hospitality in his laboratory and for the phage cultures.

**Registry No.** Lysozyme, 9001-63-2.

References

Chothia, C. (1975) *Nature (London) 254*, 304–308.
Dautry-Varsat, A., & Garel, J. R. (1978) *Proc. Natl. Acad. Sci. U.S.A. 75*, 5979–5982.
Dautry-Varsat, A., & Garel, J. R. (1981) *Biochemistry 20*, 1396–1401.
Elwell, M., & Schellman, J. A. (1975) *Biochim. Biophys. Acta 386*, 309–313.
Elwell, M., & Schellman, J. A. (1977) *Biochim. Biophys. Acta 494*, 367–383.
Garel, J. R., & Baldwin, R. L. (1973) *Proc. Natl. Acad. Sci. U.S.A. 72*, 2002–2005.
Ghélis, C. (1980) *Biophys. J. 10*, 503–514.
Ghélis, C., & Yon, J. M. (1979) *C. R. Hebd. Seances Acad. Sci., Ser. D 289*, 197–199.
Ghélis, C., & Yon, J. M. (1982) *Protein Folding*, Academic Press, New York.
Ghélis, C., Tempête-Gaillourdet, M., & Yon, J. M. (1978) *Biochem. Biophys. Res. Commun. 84*, 31–36.
Goldberg, M. E. (1972) in *Dynamics Aspects of Conformation Changes in Biological Macromolecules* (Sadron, C., Ed.) pp 57–65, Reidel Publishing Co., Dordrecht, Netherlands.
Greenfield, N., & Fasman, G. (1969) *Biochemistry 8*, 4108–4116.
Hagerman, P. J. (1977) *Biopolymers 16*, 731–747.
Högberg-Raibaud, A., & Goldberg, M. E. (1977a) *Proc. Natl. Acad. Sci. U.S.A. 74*, 442–446.
Högberg-Raibaud, A., & Goldberg, M. E. (1977b) *Biochemistry 16*, 4016–4020.
Ikai, A., & Tanford, C. (1973) *J. Mol. Biol. 73*, 145–154.
Janin, J. (1979) *Bull. Inst. Pasteur (Paris) 77*, 337–373.
Kauzmann, W. (1959) *Adv. Protein Chem. 14*, 1–64.
Kübicek, M., & Visnak, K. (1974) *Chem. Eng. Commun. 1*, 291–296.
Levitt, M., & Chothia, C. (1976) *Nature (London) 261*, 552–557.
Littman, B. J. (1966) Ph.D. Thesis, University of Oregon, Eugene, OR.
London, J., Skrzynia, C., & Goldberg, M. E. (1974) *Eur. J. Biochem. 47*, 409–415.
Mac Lachlan, A. D. (1980) *Regensburg Symposium on Protein Folding* (Jaenicke, R., Ed.) Elsevier/North-Holland Biomedical Press, New York.
Matheson, R. R., & Scheraga, H. A. (1978) *Macromolecules 11*, 819–829.
Matthews, B. W., & Remington, S. J. (1974) *Proc. Natl. Acad. Sci. U.S.A. 71*, 4178–4182.
Miles, E. W., Yutani, K., & Ogashara, K. (1982) *Biochemistry 21*, 2586–2592.
Nall, B. T., Garel, J. R., & Baldwin, R. L. (1978) *J. Mol. Biol. 118*, 317–330.
Nozaki, Y. (1970) *Methods Enzymol. 26*, 43–54.
Pace, N. C. (1975) *CRC Crit. Rev. Biochem. 3*, 1–43.
Pace, N. C., & Tanford, C. (1968) *Biochemistry 7*, 198–203.
Remington, S. J., Anderson, W. F., Owen, J., Ten Eyck, L. L., Grainger, C. T., & Matthews, B. W. (1978) *J. Mol. Biol. 118*, 81–98.
Reutimann, H., Straub, B., Luisi, P. L., & Holmgren, A. (1981) *J. Biol. Chem. 256*, 6796–6803.
Rossmann, M. G., & Argos, P. (1981) *Annu. Rev. Biochem. 50*, 497–532.
Rowe, E. S., & Tanford, C. (1973) *Biochemistry 12*, 4922–4927.
Slaby, I., & Holmgren, A. (1979) *Biochemistry 18*, 5584–5591.
Tanford, C. (1968) *Adv. Protein Chem. 23*, 121–282.
Tanford, C. (1970) *Adv. Protein Chem. 24*, 1–95.
Tanford, C., Aune, K., & Ikaï, A. (1978) *J. Mol. Biol. 73*, 185–197.
Teale, J. M., & Benjamin, D. C. (1976a) *J. Biol. Chem. 251*, 4603–4608.
Teale, J. M., & Benjamin, D. C. (1976b) *J. Biol. Chem. 251*, 4609–4615.
Teale, J. M., & Benjamin, D. C. (1977) *J. Biol. Chem. 252*, 4521–4526.
Timchenko, A. A., Ptitsyn, O. B., Dolgikh, D. A., & Fedorov, B. A. (1978) *FEBS Lett. 88*, 105–105.
Tsugita, A., & Inouye, M. (1968) *J. Biol. Chem. 243*, 391–397.
Wetlaufer, D. B. (1973) *Proc. Natl. Acad. Sci. U.S.A. 70*, 697–701.
Wetlaufer, D. B. (1981) *Adv. Protein Chem. 34*, 61–89.
Yon, J. (1978) *Biochimie 60*, 581–591.
Zetina, C. R., & Goldberg, M. E. (1980) *J. Mol. Biol. 137*, 401–414.
Zetina, C. R., & Goldberg, M. E. (1982) *J. Mol. Biol. 157*, 133–148.
Zilber, E. (1979) These 3ème Cycle, Universitē Orsay, France.